PRAMANA
— journal of
physics

Vol. 59, No. 3
September 2002
pp. 445–456

Occurrence of stable periodic modes in a pendulum with cubic damping

K I THOMAS and G AMBIKA*
Department of Physics, Maharaja's College, Cochin 682 011, India
*Email: nalanda4@satyam.net.in

MS received 2 November 2001; revised 11 March 2002

Abstract. Dynamical systems with nonlinear damping show interesting behavior in the periodic and chaotic phases. The Froude pendulum with cubical and linear damping is a paradigm for such a system. In this work the driven Froude pendulum is studied by the harmonic balancing method; the resulting nonlinear response curves are studied further for resonance and stability of symmetric oscillations with relatively low damping. The stability analysis is carried out by transforming the system of equations to the linear Mathieu equation.

Keywords. Harmonic balance; Mathieu equation; Froude pendulum; resonance.

PACS Nos 05.45.-a; 05.45.Ac; 05.45.Gg; 45.10.-b

1. Introduction

Nonlinear pendulum systems with regular and chaotic dynamics serve as classic models for the analysis of nonlinear phenomena. The Froude pendulum (FP) is one such mechanical system [1–3] involving a pendulum mounted on a rotating shaft which introduces an additional nonlinearity due to dry friction between the shaft and the pivot of the pendulum. This leads to generation of self excited limit cycles [4] in the system that can be driven to chaos by adding a forcing term [5–7].

One of the analytic methods to study the transition between periodic and chaotic behavior is the Melnikov technique. The effect of parametric modulation and secondary harmonic forcing in this transition have been analyzed in detail and reported earlier by the authors [5,7]. A survey of the periodic and chaotic regimes of the pendulum has recently been analyzed in detail by Dai and Singh [8].

In the present work, the crossover from periodicity to chaos is discussed with a detailed stability analysis using Mathieu equation together with harmonic balance (HB) method. The stability studies have been reported in similar systems earlier in the literature [9,10] where approximate solutions are obtained by harmonic balance method [11,12], and stability of these solutions are studied usually using Floquet-like techniques.

The paper is organized in the following way. In §2 a description of the Froude pendulum and its complex behavior in selected domains of the system parameters are given with

the help of bifurcation diagrams, phase space plots, Poincarè sections and Lyapunov exponent. In §3 approximate solutions of the pendulum are obtained using HB method with specific attention given to the analysis of the resonance curves. Section 4 is devoted to discussion of the stability of the periodic modes of the driven Froude pendulum, employing Mathieu equation. The final section contains our comments and conclusions about the stability regions of the FP in parameter space which indeed is a useful information, especially for mechanical engineering problems.

2. The Froude pendulum

The Froude pendulum is essentially a pendulum suspended from a dry horizontal shaft of circular cross-section by a ring or loop [1–3]. When the shaft rotates with suitable constant angular velocity ω_0, the pendulum oscillates with gradually increasing amplitude, which reaches an ultimate value. The differential equation of motion with a sinusoidal driving torque is of the type

$$\ddot{\theta} + 2\kappa(\dot{\theta}) + A\sin\theta = f\cos\omega t, \tag{1}$$

where $2\kappa(\dot{\theta})$ is the viscous damping.

The motion guided by (1) may eventually be led to limit cycle behavior when the amplitude decay due to viscous damping is balanced by the amplitude growth due to the energy supplied by the rotating shaft to the pivot (suspension) [1,3] or the motion shall become chaotic. Under this condition, (1) takes the form of the FP equation

$$\ddot{\theta} + q_1\dot{\theta}[q_2\dot{\theta}^2 - 1] + A\sin\theta = G(\omega_0) + f\cos\omega t, \tag{2}$$

where $G(\omega_0)$ is a constant torque; q_1 and q_2 are the coefficients of linear and cubic damping.

Figures 1a–d depicts the complex behavior of the pendulum in selected parameter regions. Here the restoring couple is taken as $\sin\theta$ by putting $A = 1$ and the constant torque $G(\omega_0)$ is assumed to be zero. Figure 1a is the bifurcation diagram where the angular velocity of the pendulum $(\dot{\theta})$ is plotted against the drive amplitude (f) stroboscopically. The numerical analysis is done using fourth-order Runge–Kutta–Gills algorithm and the first 200 (500 in some cases) drive cycles are neglected for settling of transients. In figures 1b and 1c the phase space plots for two f values showing the chaotic and periodic states respectively are shown. Variation of the maximal Lyapunov exponent (λ) as a function of f is shown in figure 1d.

3. Analysis using harmonic balance method

Approximate solutions for the amplitude of harmonic oscillations undergone by the FP can be obtained by the method of harmonic balance [11,12]. We assume a steady state solution for the FP equation (2) as

$$\theta_0(t) = \alpha + \beta\sin(\omega t + \phi), \tag{3}$$

with the periodicity condition

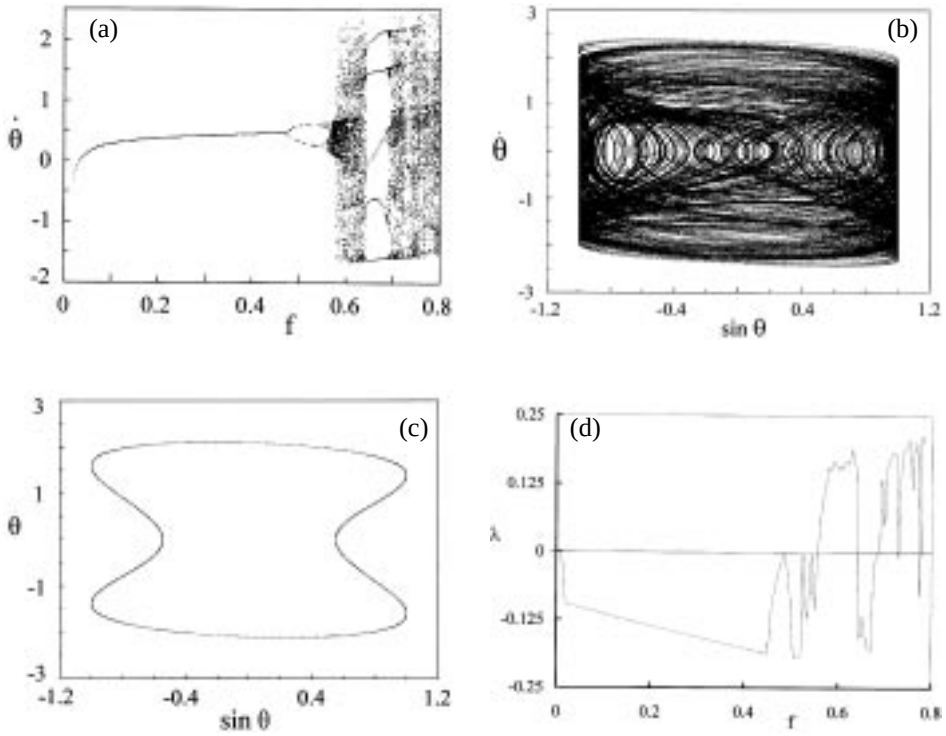

Figure 1. (**a**) Bifurcation diagram of the FP for $q_1 = 0.2,\ q_2 = 0.435, \omega = 0.7$. The velocity $\dot{\theta}$ is plotted as a function of the drive amplitude f. Chaotic behavior sets in at $f \approx 0.56$. (**b,c**). The phase space plots of the pendulum for the same q_1, q_2, ω values as in (**a**). The chaotic behavior for $f = 0.6$ is shown in (**b**) and periodic behavior for $f = 0.4$ is shown in (**c**). In (**b**) and (**c**) $\dot{\theta}$ is plotted against $\sin\theta$. The variation of the maximal Lyapunov exponent λ is plotted as a function of f in (**d**). The transition from periodic to chaotic region at $f \approx 0.56$ can be seen.

$$\theta_0(t) = \theta_0(t+\tau) = \theta_0(t+m\tau),$$

where $\tau = 2\pi/\omega$ is the period of the drive term and m an integer. Substituting (3) in (2), retaining terms up to $n = 2$ only in the Bessel expansion for $\sin(\sin)$ and equating the coefficients of $\sin(\omega t)$, $\cos(\omega t)$ and constant terms on either side of the equation, we get

$$A\sin\alpha J_0 = G(\omega_0) = G, \tag{4}$$

$$(2A\cos\alpha J_1 - \beta\omega^2)^2 + \left(q_1\beta\omega - \frac{3q_1q_2\beta^3\omega^3}{4}\right)^2 = f^2, \tag{5}$$

$$\frac{\beta(q_1\omega - 3q_1q_2\beta^2\omega^3/4)}{(2A\cos\alpha J_1 - \beta\omega^2)} = \tan\phi, \tag{6}$$

where J_n stands for $J_n(\beta)$, the Bessel functions of the first kind. With the constant torque absent ($G = 0$) three distinct possibilities can arise here by (4): (i) $\alpha = 0$, corresponding

to symmetric oscillations; (ii) $0 < |\alpha| < \pi$, corresponding to asymmetric oscillations with $\beta = \beta_s$ where $J_0(\beta_s) = 0$ and (iii) $\alpha = \pi$, corresponding to inverted symmetric oscillations. The error involved in the approximation (3) is obtained by comparing the frequency $\omega_{\rm f}$ of free oscillations of (2) for $q_1 = q_2 = f = \alpha = G = 0$ with the exact frequency $\omega_{\rm e}$. In addition to these, taking $A = 1$ in (4)–(6)

$$\omega_{\rm f}^2 = \frac{2}{\beta} J_1(\beta) = \Omega = 1 - \frac{\beta^2}{8} + \frac{\beta^4}{192} + \cdots. \tag{7}$$

The exact frequency is given by

$$\omega_{\rm e}^2 = \left[\frac{2}{\pi} K\left(\sin\frac{\beta}{2}\right)\right]^{-2} = 1 - \frac{\beta^2}{8} + \left(\frac{\beta^4}{192}\,\frac{7}{8}\right) + \cdots, \tag{8}$$

where K is an elliptic integral of the first kind [3,13]. It can be shown that the error in (7) is small and is of second order in the amplitude of the third harmonic in (3). Including higher harmonics in (3), more accurate results can be obtained.

Setting $\alpha = 0$, eq. (5) can be solved numerically, for symmetric oscillations in the harmonic amplitude β. Thus with $A = 1$ and $\alpha = 0$ in (5), we obtain

$$(2J_1(\beta) - \beta\omega^2)^2 + \left(q_1\beta\omega - \frac{3q_1q_2\beta^3\omega^3}{4}\right)^2 = f^2. \tag{9}$$

This can be rewritten with the help of (7) as

$$\beta^2(\Omega - \rho)^2 + \left(q_1\beta\omega - \frac{3q_1q_2\beta^3\omega^3}{4}\right)^2 = f^2 \tag{10}$$

where $\rho = \omega^2$. At resonance the two frequencies coincide (i.e., $\Omega = \rho$) corresponding to $\phi = \pi/2$. Hence

$$f_{\rm res} = q_1\beta\omega - \frac{3q_1q_2\beta^3\omega^3}{4}. \tag{11}$$

The drive amplitude at resonance $f_{\rm res}$ has a maximum f_* corresponding to $\mathrm{d}f_{\rm res}/\mathrm{d}\beta = 0$. Only below f_* resonance is possible. Thus the upper limit of drive amplitude for resonance is

$$f_* = \frac{4q_1}{9\sqrt{q_2}}, \qquad \beta_* J_1(\beta_*) = \frac{2}{9q_2}. \tag{12}$$

The corresponding frequency is given by

$$\omega_* = \frac{2}{3\beta_*\sqrt{q_2}}. \tag{13}$$

The variation of the amplitude $|\beta|$ with the drive frequency ω is shown in figures 2a,b. If $f < f_*$, the resonance curve has lower and upper branches ($\beta < \beta_*$ and $\beta > \beta_*$ in figure 2b). The lower branch is similar to the typical response curves for a soft-spring oscillator.

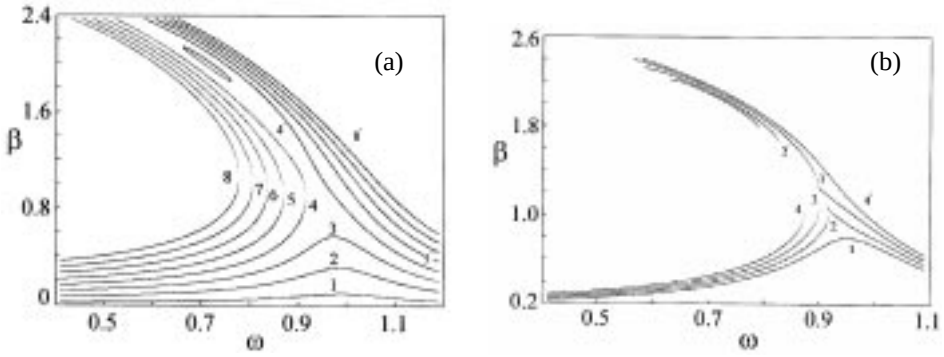

Figure 2. The response diagrams: The amplitude β of the FP oscillations is shown as a function of the drive frequency ω, for $q_1 = 0.2$, $q_2 = 0.435$. Colored portions of the curve correspond to unstable oscillations and the black sections represent stable oscillations. (**a**) The response curves for $f = 0.08, 0.1, \ldots (0.02), 0.22$ are labelled $1, 2, \ldots, 8$. Curves 4 to 8 comprise of nonjoint left and right branches; their right branches are labelled $4', 5', \ldots 8'$. (**b**) Curves for $f = 0.094, 0.114, 0.134\ (f_*), 0.154$. Resonance jump can be seen in 2 and 3. Here $1, 2, 3$ comprise of the lower branches bearing the labels and closed loop (bubble)-like upper branches labelled $1', 2', 3'$. Resonance is possible for these curves. Curve 4 is for $f > f_*(= 0.134)$ and this is disjoint.

If q_1 and q_2 are sufficiently small and if f/f_* is close to unity, this branch is triple valued between the turning points corresponding to $\mathrm{d}\omega/\mathrm{d}\beta = 0$. These turning points correspond to hysteresis jumps. The right turning point (C_1) is a saddle node fold where a jump takes place to resonance under increasing ω. Similarly when ω decreases, hysteresis jump from resonance takes place at the left turning point (C_2) corresponding to another fold [14]. In the region of this hysteresis between the folds, two harmonic steady states exist: the large amplitude resonant attractor and the low amplitude nonresonant attractor. The lower segment connecting C_1 and C_2 is an unstable saddle cycle, the stable manifold of which is the separatrix between the basins of the resonant and nonresonant attractors. The upper branch develops a bubble structure as f increases. Depending on the magnitudes of q_1 and q_2, one or more bubbles have been observed (figure 2b). The lower segment of this bubble consists of only unstable points. In the upper segment, regions below $\beta = \beta_s$ are stable while those above β_s are unstable; β_s corresponds to a symmetry breaking bifurcation. Nevertheless, in simulations by numerical integration these stable regions are difficult to materialise because the lower nonresonant segment in the response curve has a much larger basin of attraction.

When $f > f_*$, the resonance curve consists of two separate branches. The lower branch is stable below the (only one) turning point and unstable above that. In the upper branch states above β_s are unstable and below are stable due to a symmetry breaking bifurcation, as in the case for $f < f_*$.

The values of β_*, f_*, and ω_* for different q_2 values are plotted in figure 3. The minimum value of q_2 above which only resonance can take place is given by

$$q_{2\,\mathrm{min}=} \frac{2}{9(\beta_* J_1(\beta_*))_{\mathrm{max}}} = 0.1781. \tag{14}$$

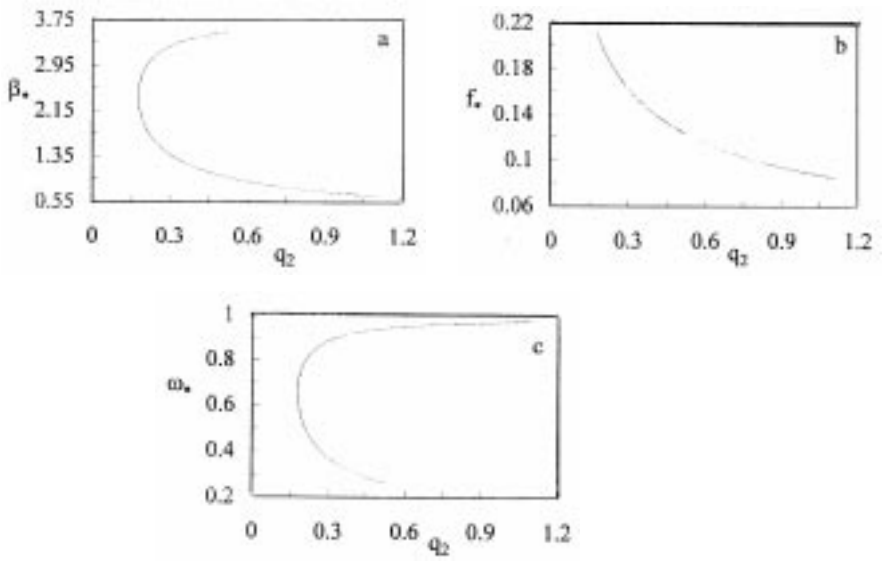

Figure 3. Variation of the quantities β_*, f_* and ω_* plotted in (**a**), (**b**), and (**c**) respectively against q_2 for $q_1 = 0.2$. Existence of $q_{2\min}(\approx 0.178)$ can be seen in all the three diagrams.

Condition for the resonance curve (5) to have a maximum $\beta = \beta_0$ is

$$\frac{27}{16}q_1^2q_2^2\rho^2\beta^4 - 3q_1^2q_2\rho\beta^2 + 2(\rho - \Omega) + q_1^2 = 0.$$

The values of $\rho = \rho_0$ for which response amplitude β is maximum (β_0) is given by solutions of the equation

$$\rho_0 = \frac{8(3q_1^2q_2\beta^2 - 2)}{27q_1^2q_2^2\beta^4} \pm \frac{8\left\{\left(3q_1^2q_2\beta^2 - 2\right)^2 - (27/4)q_1^2q_2^2\beta^4\left(q_1^2 - 2\Omega\right)\right\}^{1/2}}{27q_1^2q_2^2\beta^4}. \tag{15}$$

In general, this ρ_0 is two valued (ρ_{0_1}, ρ_{0_2}) suggesting the existence of two maxima for the resonance curves. These two maxima may coincide giving a single maximum if $\rho_{0_1} = \rho_{0_2}$, the condition for which is

$$(3q_1^2q_2\beta^2 - 2)^2 = \frac{27}{4}q_1^2q_2^2\beta^4\left(q_1^2 - 2\Omega\right). \tag{16}$$

The general conditions for the ρ values to coincide for any β can be obtained by treating (10) as an equation in ρ. There are two necessary conditions for this, of which one is the same as (16) and the other is

$$f^2 = \Omega^2\beta^2 - \frac{32(2 - 3q_1^2q_2\beta^2)^3}{3^7q_1^4q_2^4\beta^6}. \tag{17}$$

The maximum value of the drive amplitude f, below which only ρ's coincide and β is maximum is given by

$$f_x = 2J_1(\beta), \qquad q_1^2 = \frac{4J_1}{\beta}. \tag{18}$$

The condition (18) is obtained using the fact that ρ should not be negative. Then f_x has the maximum value 1.164 at $\beta_x = 1.841$ corresponding to $q_{1_x} = 1.124$. It is observed that in general f_x is less than f_*.

4. Stability analysis of the solutions

The solutions (5) of the FP obtained by harmonic analysis can be tested for stability by applying a small perturbation $\delta\theta$ to the assumed steady state solutions (3). With $A = 1$ and $G = 0$, the variational equation for the FP (2) is given by

$$\delta\theta'' + 3q_1q_2\theta_0'^2\delta\theta' - q_1\delta\theta' + \cos\theta_0 \sin(\delta\theta_0) = 0. \tag{19}$$

Here prime stands for differentiation with respect to time t. Assuming the disturbance $\delta\theta$ to be of the form

$$\delta\theta = \mathrm{e}^{v(t)}u(t), \tag{20}$$

where $u(t)$ is a periodic function in t, the variational equation takes the form

$$u'' + u'\left(2v' + 3q_1q_2\theta_0'^2 - q_1\right) + u\left(v'' + v'^2 + 3q_1q_2\theta_0'^2v' - q_1v' + \cos\theta_0\right) = 0. \tag{21}$$

The stability of the solutions depends primarily on the function $v(t)$. The essential condition for asymptotic stability is that $v(t)$ should be negative. On substituting for θ from (3), (21) gives

$$\begin{aligned}\ddot{u} + \dot{u}\left\{2\dot{v} - (q_1/\omega) + 3q_1q_2\beta^2\omega/2 + (3q_1q_2\beta^2\omega\cos 2\tau')/2\right\} \\ + u\{\dot{v}^2 + \ddot{v} - q_1\dot{v}\left((1/\omega) - 3q_2\beta^2\omega/2\right) + (3q_1q_2\beta^2\omega\dot{v}\cos 2\tau')/2 + J_0/\omega^2 \\ + 2J_2(\cos 2\tau')/\omega^2\} = 0,\end{aligned} \tag{22}$$

where dot denotes differentiation with respect to $\tau' = \omega t + \phi$.

The equation can be brought to the form of standard (linear) Mathieu equation [15], if the coefficient of $\dot{u}$ vanishes. This happens when

$$v = \left(\frac{q_1}{2\omega} - \frac{3q_1q_2\beta^2\omega}{4}\right)\tau - \frac{3q_1q_2\beta^2\omega\sin 2\tau'}{8}. \tag{23}$$

The assumed solution (3) can be stable only if v is negative. From this condition we define a critical amplitude $\beta_c = \sqrt{2/3q_2\omega^2}$ below which only the oscillations are bounded. If q_1 is negative, the condition just reverses. In short, for stable oscillations $\beta < \beta_c$ $(> \beta_c)$ for $q_1 > (<)0$. Incorporating this restriction, (22) gets modified as

$$\ddot{u} + u\{a + 2q\cos(2\tau)\} = 0 \tag{24}$$

with

$$a = \frac{J_0}{\omega^2},$$
$$q = \frac{1}{2}\{(2J_2/\omega^2)^2 + (3q_1q_2\beta^2\omega/2)^2\}^{1/2},$$
$$\tau = \omega t + \left(\phi + \frac{\pi}{2} - \frac{\varepsilon}{2}\right),$$

and

$$\varepsilon = \arctan\left(3q_1q_2\beta^2\omega^3/4J_2\right).$$

The stability analysis can further be carried out by perturbation method [3,16]. When q is small, expanding u and a of (24) in power series in q

$$u(\tau) = u_0(\tau) + qu_1(\tau) + q^2u_2(\tau) + \cdots + q^nu_n(\tau),$$
$$a(q) = a_0 + qa_1 + q^2a_2 + \cdots + q^na_n. \tag{25}$$

Here the perturbation series in a is required for eliminating the secular terms arising while solving for $u_n(\tau)$, $n = 1, 2, \ldots$. Substituting (25) in (24), taking terms of the same order in q and equating to zero, we get

$$u_0'' + a_0u_0 = 0. \tag{26}$$

$$u_1'' + a_0u_1 + a_1u_0 - 2\cos(2\tau)u_0 = 0. \tag{27}$$

and

$$u_2'' + a_0u_2 + a_1u_1 + a_2u_0 - 2\cos(2\tau)u_1 = 0. \tag{28}$$

In (26)–(28) primes denote differentiation with respect to τ. Equation (28) can be solved for u_0. This gives

$$u_0 = A_0\cos\sqrt{a_0}\tau + B_0\sin\sqrt{a_0}\tau \tag{29}$$

where A_0 and B_0 are constants to be determined from initial conditions. Generally solutions of periodicity π or 2π are sought and this depends in this case on the values of a through a_0, a_1, etc.. Hence we differentiate the following three cases of lowest values of a_0.

4.1 *Case A*

$a_0 = 1$:
With this restriction (29) gives

$$u_0 = A_0\cos\tau + B_0\sin\tau. \tag{30}$$

The solution is periodic with period 2π. Substituting this value in (27), the differential equation for u_1 is obtained

$$u_1'' + u_1 = -(a_1 - 1)A_0 \cos\tau - (a_1 + 1)B_0 \sin\tau + A_0 \cos 3\tau + B_0 \sin 3\tau. \quad (31)$$

The first two terms on the right side cause secular growth of the solutions. Either of these can be removed by fixing a_1 properly. Accordingly

(i) When $a_1 = 1$ the first term goes, and we get

$$u_1 = A_1 \cos\tau + B_1 \sin\tau - \frac{1}{8}\left\{A_0 \cos 3\tau + B_0 \sin 3\tau\right\} + B_0 \tau \cos\tau,$$

A_1 and B_1 being constants depending on A_0 and B_0.

The first three terms when combined together give a period 2π oscillation; the last term is unbounded and hence causes instability. Now by (25) the boundary for transition from stable to unstable mode is located at

$$a = 1 + q \equiv M(1). \quad (32)$$

(ii) When $a_1 = -1$ the second term in (31) vanishes to give a general solution

$$u_1 = A_1 \cos\tau + B_1 \sin\tau - \frac{1}{8}\left\{A_0 \cos 3\tau + B_0 \sin 3\tau\right\} + A_0 \tau \cos\tau. \quad (33)$$

The situation is similar to that for $a_1 = 1$, except that the corresponding stability boundary is

$$a = 1 - q \equiv N(1) \quad (34)$$

where the functions labelled $M(i)$ and $N(i)$ in (32) and (34) respectively are truncated forms of the Mathieu functions with $i = \sqrt{a_0}$ [3], for q small enough and relevant for solutions of period π and 2π.

A point exactly on the transition boundary gives rise to a solution with a periodic stable part and a growing unstable part. The boundary is therefore unstable in general.

4.2 *Case B*

When $a_0 = 4$ in (29), the general solution is

$$u_0 = A_0 \cos 2\tau + B_0 \sin 2\tau. \quad (35)$$

It is obvious that this equation gives a period π solution. With this (27) becomes

$$u_1'' + 4u_1 = -a_1\left(A_0 \cos 2\tau + B_0 \sin 2\tau\right) + A_0 + A_0 \cos 4\tau + B_0 \sin 4\tau.$$

The first term here causes secular growth. On taking $a_1 = 0$, this can be removed. This results in

$$u_1 = A_1 \cos 2\tau + B_1 \sin 2\tau + \frac{A_0}{4} - \frac{1}{12}\left(A_0 \cos 4\tau + B_0 \sin 4\tau\right). \quad (36)$$

Rewriting (28) using (36), we get

$$u_2'' + 4u_2 = -\left(a_2 - \frac{5}{12}\right) A_0 \cos 2\tau - \left(a_2 + \frac{1}{12}\right) B_0 \sin 2\tau + A_1 (1 + \cos 4\tau) + B_1 \sin(4\tau) - \frac{1}{12}\left(A_0 \cos 6\tau + B_0 \sin 6\tau\right). \quad (37)$$

Here the two harmonic terms in 2τ cause secular growth. Either of these (not both, simultaneously) can be removed by suitable choice of a_2. Thus, when $a_2 = \frac{5}{12}$, first term vanishes; if $a_2 = -\frac{1}{12}$, the second term goes. Correspondingly the transition boundaries in the $a - q$ plane, are given by

$$\text{(i)} \qquad a = 4 + \frac{5}{12} q^2 \equiv M(2) \quad \text{for} \, a_2 = \frac{5}{12}$$

$$\text{(ii)} \qquad a = 4 - \frac{1}{12} q^2 \equiv N(2) \quad \text{for} \, a_2 = -\frac{1}{2}. \quad (38)$$

4.3 *Case C*

Taking $a_0 = 0$, the differential equation (26) for the zeroth order solution u_0 gives $u_0'' = 0$, the solution for which has the form

$$u_0 = A_0 + B_0 \tau.$$

Neglecting $B_0 \tau$, the term which grows unbounded as $t(\tau) \to \infty$ we obtain

$$u_0 = A_0. \quad (39)$$

Using this in (27) the equation for u_1 becomes

$$u_1'' = -a_1 A_0 + 2A_0 \cos 2\tau.$$

Secular growth in this solution due to the presence of constant term can be checked by putting $a_1 = 0$. The resulting bounded solution is

$$u_1 = -\frac{A_0}{2} \cos 2\tau. \quad (40)$$

This is a period π solution. Now considering (28), to avoid secular growth, a_2 should be $-\frac{1}{2}$. Consequently the transition boundary becomes

$$a = -\frac{q^2}{2} \equiv M(0). \quad (41)$$

Regions with $a \in (M(0), N(1))$, $a \in (M(1), N(2)$ and $a \in (M(2), N(3))$ are stable. The unstable regions correspond to $a \in (M(1), N(1))$, $a \in (M(2), N(2))$ and $a < M(0)$. Solutions with $a = M(0), \ldots, N(2)$ are in general unstable. The regions of stable solutions based on all the three cases above, are marked in figure 4 in a f–ω parameter plane. Here the regions with stable solutions (depending on the number of coexisting solutions) and unstable solutions are marked differently.

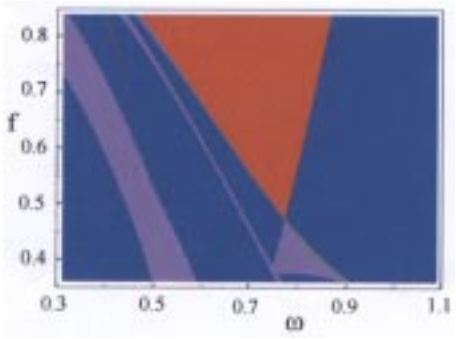

Figure 4. Regions of stable and unstable solutions, differentiated by Mathieu equation analysis in the f–ω plane. Regions in blue correspond to one stable solution while purple regions correspond to two stable solutions. Regions with three stable solutions coexisting are shown in green color and the red regions correspond to unstable solutions.

5. Conclusion

In this paper we have studied the dynamics of the Froude pendulum by harmonic balancing method. The regions of resonance are identified with respect to the amplitude and frequency of the periodic forcing. With the help of standard tools like bifurcation diagrams, p.s plots and their Poincarè sections and Lyapunov exponents regions in parameter space where stable and unstable oscillations occur have been identified, numerically. Analytic study of the pendulum with regard to stability has been done in the ω–f plane by transforming the nonlinear equation of the FP to a (linear) Mathieu equation.

It is found that the regions predicted by the Mathieu equation analysis almost coincide with the ones identified by the numerical study. Thus for $\omega = 0.7$ the LCE plot shows that regions in $f < 0.56$ as stable. This is also suggested by the bifurcation diagram (figure 1a). The prediction by the Mathieu equation analysis shown in figure 4 agrees with this. But the analytical study is restricted to only the symmetric oscillations. Further, the results of the analysis will be error free only below f_* and β_*. A more accurate study by including higher harmonics in (3) and higher order Bessel functions in (5) can extend the results to almost the complete parameter space.

References

[1] N Minorsky, *Nonlinear oscillations* (Van Nostrand, Princeton, NJ, 1962)
[2] S P Streklov, *Z. Tech. Fiz.* **11**, 93 (1933)
[3] N W Maclachan, *Ordinary nonlinear differential equations in engineering and physical sciences* (Oxford University Press, 1956)
[4] H T Davis, *Introduction to nonlinear differential and integral equations* (Dover Publications Inc., NY, 1960)
[5] K I Thomas and G Ambika, *Pramana – J. Phys.* **52**(4), 375 (1999)
[6] K I Thomas and G Ambika, in *Computational aspects in chaos and nonlinear dynamics* edited by G Ambika and V M Nandakumaran (Wiley Eastern, New Delhi, 1994)

[7] K I Thomas and G Ambika, in *Nonlinear dynamics – integrability and chaos* edited by M Daniel, K M Thamizhmakan and R Sahadevan (Narosa, New Delhi, 2000)
[8] L Dai and M C Singh, *Int. J. Nonlinear Mech.* **33**, 947 (1998)
[9] D D′Humieres, M R Beasley, B A Huberman and A Libchaber, *Phys. Rev.* **A26**, 3483 (1982)
[10] S Narayanan and K Jayaraman, *J. Sound Vib.* **146**, 17 (1991)
[11] R E Mickens, *J. Sound Vib.* **94**, 456 (1984)
[12] R E Mickens, *J. Sound Vib.* **111**, 518 (1986)
[13] J Miles, *Physica* **D31**, 252 (1998)
[14] J M T Thompson and M S Soliman, *Proc. R. Soc. London* **A432**, 101 (1991)
[15] T L Saty and J Bram, *Nonlinear mathematics* (McGraw-Hill Inc., NY, 1964)
[16] A H Nayfeh, *Introduction to perturbation techniques* (Wiley-Interscience, NY, 1981)